Database of the hydrogen sulfide absorption in the 4400–11400 cm^{-1} region

O.V. Naumenko and E.R. Polovtseva

Institute of Atmospheric Optics,
Siberian Branch of the Russian Academy of Sciences, Tomsk

Received September 22, 2003

Detailed rovibrational absorption spectrum of the H_2S molecule is calculated in the 4400–11400 cm^{-1} spectral region. The present compilation is based on the theoretical analysis of the high-resolution Fourier-transform spectra recorded at the Kitt Peak National Observatory (USA) and the intracavity spectra recorded at the Josef Fourier University, Grenoble, France. The spectrum comprises about 29 000 lines with the intensities exceeding 10^{-7} cm^{-2} atm^{-1} for the FT spectra and in excess of $2 \cdot 10^{-9}$ cm^{-2} atm^{-1} for the intracavity spectra. These lines belong to 59 vibrational bands of the $H_2{}^{32}S$, $H_2{}^{33}S$, and $H_2{}^{34}S$ molecules including some hot bands originating from the (010) state. In the case of the FT spectra (4400–8040 cm^{-1}), line positions are calculated from the experimental upper energy levels accurate to within 0.0001–0.015 cm^{-1}. Line intensities for the FT spectra were calculated using the transformed transition moment parameters retrieved from fitting to experimental data for the cold bands of the $H_2{}^{32}S$ molecule. The accuracy of calculated line intensities varies from 3 to 20%. The experimental positions and calculated intensities are presented in the database for the intracavity spectra (9400–11400 cm^{-1}); the measurement accuracy is 0.003–0.025 cm^{-1} for line positions and 20–30% for line intensities.

Introduction

The study of absorption spectra of H_2S is important, because using such information it is possible to determine the presence and concentration of hydrogen sulfide in the atmosphere. It is also important for spectroscopic provision of atmospheric sensing, as well as for applications to atmospheric chemistry of Venus and other planets.

From the theoretical point of view, the hydrogen sulfide molecule is of great interest, since it is an example of a light asymmetric top, for which the nuclei motion can be perturbed by strong intramolecular interactions arising at vibrational and rotational excitation. The H_2S energy spectrum was modeled in many papers with the use of various theoretical approaches to demonstrate the effects of localization of vibrational excitation or vibrational-rotational interaction. High overtone vibrations in H_2S are almost independent of each other, thus creating the possibility of local vibrational excitation of an individual molecular bond, which is a key to control over chemical reactions.

In addition, the data on H_2S absorption spectra are of great interest from both practical and theoretical points of view, almost no information about the H_2S absorption spectra in the region above 4300 cm^{-1} can be found in the known databases, such as HITRAN and GEISA. The problem of compilation, verification, and improvement of databases on the absorption spectra of the most of atmospheric constituents and pollutants has been recognized quite urgent, for example, in reports and discussions at the Atmospheric Spectroscopy Applications Workshop held in Moscow, Russia in 2002. Thus, Professor P. Varanasi, Institute for Terrestrial and Planetary Atmospheres, USA, emphasized that improvements made to the databases in recent four decades are only a drop, though significant, in the ocean of atmospheric spectroscopy.

Modern databanks of spectroscopic information cannot be compiled without adequate mathematical modeling of the positions and intensities of the spectral lines. As known, precision routine measurements of intensities are quite difficult, especially, in the case of weak absorption lines. At the same time, the total contribution of weak lines to the integral absorption of radiation by hydrogen sulfide may be large enough in some spectral intervals. In this situation, it is very important to have the possibility of calculating the high-accuracy and detailed absorption spectra.

Based on the rotational, centrifugal distortion, and resonance parameters as well as the dipole moment constants retrieved from analysis of experimental Fourier-transform spectra,[1–3] we have compiled the database on H_2S absorption in the 4400–8040 cm^{-1} region. Since the accuracy of calculated spectra included into the database is an important characteristic, a particular attention has been paid to the methods and quality of retrieval of spectroscopic parameters that make up the foundation for calculations. In addition to the synthetic spectrum in the 4400–8040 cm^{-1} region, the database includes recently published[4,5] experimental data on the intracavity absorption spectra of hydrogen sulfide in the region from 9400 to 11400 cm^{-1}.

0235-6880/03/11 900-07 $02.00

1. Experimental spectra and their assignment

The H_2S absorption spectra in the region from 4500 to 7900 cm^{-1} were recorded by L. Brown with a Fourier-transform spectrometer at the Kitt Peak National Observatory (USA)[1–3,6] with the spectral resolution of 0.006, 0.012, and 0.021 cm^{-1}. Line positions have the accuracy characteristic of a Fourier-transform experiments, i.e., 0.0001 to 0.015 cm^{-1}. To assign the spectrum, absorption coefficients at the line peaks were roughly determined for every line. In addition, high-accuracy (2–5%) intensities were measured for 1700 lines in the 4500–5500 cm^{-1} region and 1200 lines in the 5700–6600 cm^{-1} region.

The intracavity H_2S absorption spectra in the 9400–11400 cm^{-1} region were recorded by A. Campargue, the Josef Fourier University, Grenoble, France.[4,5] The accuracy of line positions varied from 0.003 to 0.025 cm^{-1}. The intensity values for strong and medium lines were estimated with the mean accuracy of 20–30%, and it was assumed that the intensities of the weakest lines might be significantly (up to 100%) overestimated.

Experimental spectra were assigned using the program for automatic assignment of the rotational-vibrational spectra. This program based on the pattern recognition theory was developed at the Institute of Atmospheric Optics SB RAS under the financial support from the Russian Foundation for Basic Research.[7] Analysis of spectra of polyatomic molecules, in particular, the H_2S molecule is a complicated and time-consuming problem. This program tenfold decreases the time needed for assignment and allows avoiding mistakes that are inevitable at manual assignment. The program can be run both in the mode of recognition of line sets meeting a combination rule and in the mode of recognition of individual lines.

The line assignment process was performed simultaneously with the retrieval of spectroscopic parameters and controlled by the predictive calculations of line positions and intensities. Since assignment and modeling of the intracavity spectra are described thoroughly in recent papers,[4,5] let us focus here on analysis of the spectrum in the region from 4500 to 7900 cm^{-1}.

Natural hydrogen sulfide includes, in addition to the main species, significant amounts of the $H_2{}^{33}S$ (0.78%) and $H_2{}^{34}S$ (4.21%) isotopic species, what allows their spectra to be studied as well. For analysis of H_2S absorption in the 7200–7900 cm^{-1} region, we used two spectra recorded at different pressures. This favored a considerable increase in the number of assigned lines and, consequently, in the reconstructed experimental energy levels. The combined approach to assignment of the spectrum allowed us to assign 90% of $H_2{}^{32}S$, $H_2{}^{33}S$, and $H_2{}^{34}S$ absorption lines, that is, more than 12 000 lines. The high-accuracy experimental energy levels were obtained by adding the lower-state energy levels to the assigned wave numbers.[8] Table 1 summarizes the data on the experimental energy levels reconstructed from analysis of the spectrum.

Table 1. Experimental energy levels of $H_2{}^{32}S$, $H_2{}^{33}S$, and $H_2{}^{34}S$ and their accuracy

Polyad	$V_1\ V_2\ V_3$	$H_2{}^{32}S$ E_V, cm^{-1}	Number of levels		
			$H_2{}^{32}S$	$H_2{}^{34}S$	$H_2{}^{33}S$
1st hexad	0 4 0	4661.673	121		
	1 2 0	4932.699	174	62	
	0 2 1	4939.104	192	102	44
	2 0 0	5144.986	229	123	65
	1 0 1	5147.220	236	158	81
	0 0 2	5243.101	199	102	36
Total number of levels			1151	547	226
Number of fitted parameters			130	67	27
Standard deviation, cm^{-1}			0.0009	0.0011	0.0013
2nd hexad	0 5 0	5797.235	40		
	1 3 0	6074.581	117	19	
	0 3 1	6077.595	129	1	
	2 1 0	6288.146	225	128	46
	1 1 1	6289.173	246	146	88
	0 1 2	6385.299	14	1	
Total number of levels			760	285	134
Number of fitted parameters			102	36	16
Standard deviation, cm^{-1}			0.0019	0.0013	0.0009
1st decade	2 2 0	7419.916	71	14	
	1 2 1	7420.092	122	14	1
	2 0 1	7526.545	159	85	45
	1 0 2	7576.381	133	39	9
	3 0 0	7752.264	141	51	
	0 0 3	7779.319	152	44	
Total number of levels			778	247	55
Number of fitted parameters			111	31	5
Standard deviation, cm^{-1}			0.0014	0.0016	0.0023

At the final stage of the assignment, in the 4500–7900 cm^{-1} we have found absorption lines belonging to the so-called hot bands (111)–(010), (210)–(010), (121)–(010), as well as some transitions belonging to the very weak bands (012)–(000) and (220)–(000).

2. Modeling the H_2S absorption line positions and intensities

For modeling the $H_2{}^{32}S$ experimental energy levels, we used the Watson's effective rotational Hamiltonian. Interactions of the Coriolis and Darling–Dennison types were taken into account in the resonance blocks, along with the weak Fermi resonance. The H_2S absorption spectrum has a pronounced polyad structure. The spectra in the 4500–5500 cm^{-1} region are formed by transitions to the states (101), (021), (120), (040), (200), and (002) entering into the first hexad of the interacting states. Transitions to the states of the second hexad: (111), (031), (130), (210), (012), and (050), form the spectrum in the 5700–6600 cm^{-1} region. Finally, the absorption in the 7200–7900 cm^{-1} region is caused by the transitions to rotational sublevels of the states belonging to the first decade: (003), (201), (121), (102), (300), (220), (041), (022), (140), (060). Of all the vibrational states listed above, the (012), (041), (022), (140), and (060) states are "dark," that is, transitions to them are either not observed due to the low intensity or manifest themselves in a few lines borrowing intensity from strong lines – resonance partners.

For retrieval of the rotational, centrifugal distortion, and resonance parameters of the Hamiltonian, all the states of a polyad were considered simultaneously. Whenever necessary, the effect of dark states was taken into account as well. Finally, we obtained the sets of parameters allowing reconstruction of the initial experimental energy levels with high accuracy (0.0009–0.0023 cm^{-1}). The ratio of the number of levels to the number of the fitted parameters was no less than seven for all the polyads under consideration. Table 1 gives the total numbers of energy levels involved in the fitting procedure and the fitted parameters for each polyad, as well as the root-mean-square deviation of the calculated data from the experimental ones.

The correctness of the fitting is also supported by the fact that the new estimate of the vibrational energy $E_V = 6385.299$ cm^{-1} obtained in this work for the dark state (012) agrees very well with two independent calculations[9,10] in contrast to $E_V = 6388.73$ cm^{-1} from Ref. 11.

The wave functions obtained from solution of the inverse problem for the energy levels were then used to retrieve the parameters of the transformed dipole moment of the vibrational states of $H_2{}^{32}S$ analyzed by the method developed in Ref. 12. These parameters determined from fitting to high-accuracy experimental intensities are presented in Table 2 for the first hexad and in Table 3 for the second one. The obtained rms deviations of the calculated values from the measured intensities (3.10% for the first hexad and 3.35% for the second one) are close to the experimental uncertainty in the initial data.

Table 2. Parameters of transformed dipole moment for vibrational states of the 1st hexad of $H_2{}^{32}S$ (in $D \cdot M$)

N	M	(101)	(021)	(120)	(040)	(200)	(002)
1	$\cdot 10^{-3}$	–3.03999(474)	0.90134 (133)	0.46750 (122)	–0.155112(626)	2.09359(220)	0.89228(274)
2	$\cdot 10^{-6}$	–0.6858(283)	–	–0.2055(124)	–0.09422(849)	–	–0.4338(326)
3	$\cdot 10^{-5}$	0.25476(781)	–	0.06507(467)	–	–	0.1358(127)
4	$\cdot 10^{-4}$	0.21448(377)	–0.18493(203)	0.22597(158)	–0.20906(831)	–0.36962(214)	0.09279(417)
5	$\cdot 10^{-5}$	–	–	0.9466(104)	0.0454(500)	–2.3671(224)	3.1235(269)
6	$\cdot 10^{-4}$	–0.45782(300)	0.14272(163)	–	–	–	–0.013862(690)
7	$\cdot 10^{-6}$	–0.3572(342)	–	–0.4066(208)	–0.1250(129)	–	–0.1532(407)
8	$\cdot 10^{-6}$	–0.7200(273)	–	–	–	–	–
RMSD, %		2.51	2.99	3.45	4.60	3.36	3.25
Line number		470	291	154	92	355	134

Note: RMSD is the root-mean-square deviation, in %; 68% confidence intervals are given in parentheses.

Table 3. Parameters of the transformed dipole moment for vibrational states of the 2nd hexad of $H_2{}^{32}S$ (in $D \cdot M$)

N	M	(111)	(031)	(130)	(210)	(050)	(012)
1	$\cdot 10^{-3}$	–1.87165(220)	–0.166157(640)	0.211757(780)	0.81564(210)	–.060859(350)	–
2	$\cdot 10^{-7}$	–	–	–0.493(110)	–0.576(140)	–	––
3	$\cdot 10^{-6}$	0.3205(440)	–0.1888(200)	–0.3033(380)	0.1635(260)	–0.1245(250)	–
4	$\cdot 10^{-5}$	–0.2692(260)	–0.2371(110)	–0.4678(140)	0.3190(140)	0.10009(570)	–
5	$\cdot 10^{-6}$	–	–	–0.3457(880)	12.055(140)	0.1004(230)	–
6	$\cdot 10^{-4}$	–0.11209(170)	–0.010139(800)	–	–	–	–
7	$\cdot 10^{-7}$	–	–	–0.703(147)	–	–0.8890(770)	–
8	$\cdot 10^{-6}$	–0.1705(170)	–0.22317(900)	–0.0663(150)	0.1002(180)	0.0916(110)	–
RMSD, %		2.98	4.63	3.83	3.13	4.07	4.98
Line number		497	102	138	284	60	7

Note: RMSD is the root-mean-square deviation, in %; 68% confidence intervals are given in parentheses.

The adequacy of the wave functions for the dark state (012) is confirmed by the fact that the intensities of transitions of the band (012)–(000) are calculated satisfactorily, despite all parameters of the transition moment for the state (012) are zero. The good agreement, in general, between the experimental and calculated spectra for the both hexads is obvious from Fig. 1.

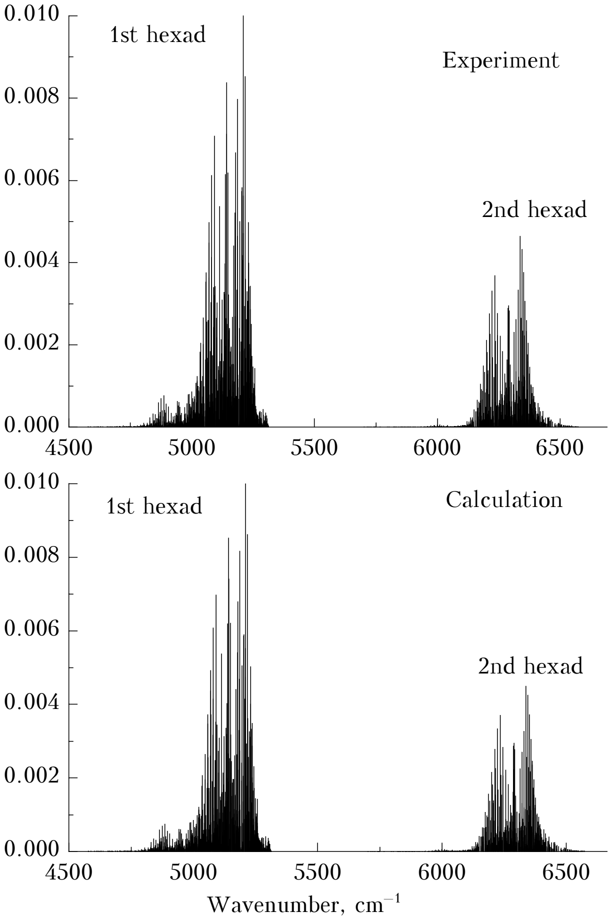

Fig. 1. Experimental and calculated absorption spectra in the region of the first and second hexads.

At the same time, it should be noted that for some transitions to the state (210) the set of parameters obtained (Table 3) does not permit reconstructing the intensities at the level of the experimental accuracy (deviations achieve 10–20%).

Although in the case of transitions to the states of the first decade the intensities were known only roughly, with the accuracy no higher than 15–20%, the parameters of the transformed transition moment for the decade states were also reconstructed from fitting to the best 931 measured values. These parameters are given in Table 4 along with the rms deviations for each state under study. Note that for the state (220) only one parameter was fitted. This is caused by the fact that lines of the (220)–(000) band more actively borrow the intensity from resonance partnering the lines of the stronger (121)–(000) band due to mixing of the wave functions. The agreement between the calculated and experimental spectra in the region of the first decade is demonstrated in Fig. 2.

Once the inverse problems on the line positions and intensities of the basic, $H_2{}^{32}S$, isotopic species were solved, it became much simpler to carry out consideration of the $H_2{}^{33}S$ and $H_2{}^{34}S$ species. The initial rotational and centrifugal distortion constants of the Hamiltonian for isotopic species were calculated from the parameters for the main isotopic species using isotopic relations:

$$A_{\text{iso}}^{V_1V_2V_3} = A_{\text{main}}^{V_1V_2V_3} \frac{A_{\text{iso}}^{000}}{A_{\text{main}}^{000}} .$$

The initial values of the resonance constants were set equal to the corresponding values of the main isotopic species. Then some parameters of $H_2{}^{33}S$ and $H_2{}^{34}S$ were refined from fitting to experimental levels.

The intensities of the isotopic H_2S absorption lines were calculated using the dipole moment parameters for the main isotopic species and normalized to the natural abundance of the corresponding species. Finally, the line intensities of the hot bands were calculated using the transition moment parameters for the corresponding cold bands.

Table 4. Parameters of transformed dipole moment for vibrational states of the 1st decade of $H_2{}^{32}S$ (in 10^{-5} D)

N	(003)	(201)	(121)	(102)	(300)	(220)
1	–19.0429(230)	46.994(190)	–21.593(220)	18.006(310)	–26.628(140)	
2	–0.01490(210)			–0.02299(330)		
3	–0.03002(780)			0.0594(100)		
4		0.5192(370)	0.4846(300)	–.4223(320)		
5			–0.4114(390)	0.5752(210)	–0.5469(180)	–0.9538(490)
6		1.6779(330)			0.03457(560)	
7			–0.10112(100)		–0.02743(390)	
8			–0.04484(430)			
RMSD, %	13.6863934	10.0060154	13.8226205	11.8127993	12.8431081	13.5276369
Line number	148	289	135	141	198	20

Note: RMSD is the root-mean-square deviation, in %; 68% confidence intervals are given in parentheses.

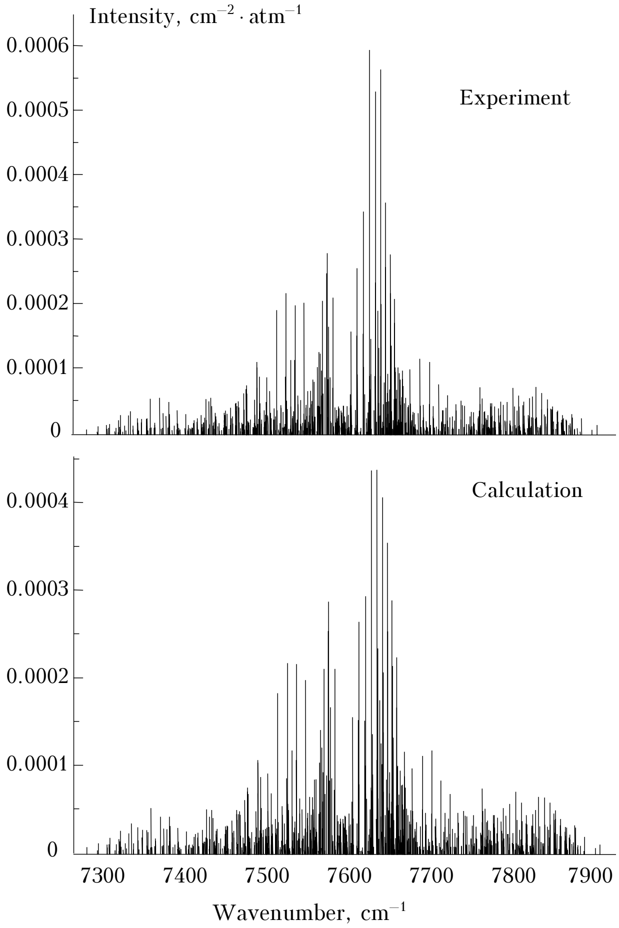

Fig. 2. Experimental and calculated $H_2{}^{32}S$ absorption spectra in the region of the first decade.

3. Database of H_2S absorption in the region from 4400 to 11400 cm^{-1}

To compile a detailed and precision database on the hydrogen sulfide absorption in the 4470–8040 cm^{-1} region, we have calculated the synthetic spectra of $H_2{}^{32}S$, $H_2{}^{33}S$, and $H_2{}^{34}S$, including hot bands. To achieve high accuracy of the calculated data, the line positions were calculated only from the experimental upper energy levels. As a result, we could estimate the accuracy of line positions in the region from 4470 to 8040 cm^{-1} of 0.0001–0.015 cm^{-1}. The intensities of all the absorption lines were calculated based on the retrieved dipole moment parameters. The database included all absorption lines with the intensity no lower than 10^{-7} cm^{-2} · atm^{-1}.

Based on the attested predictive capability of the transition moment parameters, the accuracy of the calculated intensities was estimated for cold bands of the studied isotopic species of H_2S in the region from 4470 to 8040 cm^{-1}. It was found that the accuracy of calculated intensities ΔI varied from < 5 to ≥ 20% (Table 5). As to the lines of the hot bands in this region, for them the error is greater than or equal to 20% taking into account that they were calculated using a simplified equation.

Since the precision measurements of the intensities for the Fourier-transform spectrum in the region from 7200 to 7900 cm^{-1} were not carried out, the calculated data were obtained based on the transition moment parameters retrieved from fitting to 931 roughly measured experimental values (see Table 4). In this case we achieved, using 21 fitted parameters, reconstruction of the initial data at the level of 12%. However, with regard for the large variance of the discrepancy between the calculated and experimental data (from 1 to 30%) and possible absolute error, the error for all the calculated intensities in this spectral region is equal to or more than 20%.

For the intracavity spectra in the region from 9400 to 11400 cm^{-1}, the database includes experimental positions of absorption lines and calculated intensities no lower than $2 \cdot 10^{-9}$ cm^{-2}·atm^{-1}. The accuracy of these data has been thoroughly discussed elsewhere.[4,5] It should be only noted here that the mean uncertainty in the line positions for the intracavity spectra is 0.003–0.006 cm^{-1}, as judged from the accuracy of fulfillment of the combination rule. However, if taking into account the possible absolute calibration error, the mean uncertainty in the line positions is less than 0.01 cm^{-1}. The intensities for the intracavity spectra were roughly estimated from the absorption at line peaks and then normalized to the FT data,[6] which also were approximate estimates. The accuracy of the calculated intensities for the intracavity data can be estimated as 20–30% for strong and medium lines and up to 100% for weak lines, and the intensity of the latter seems overestimated.

Table 5. Accuracy of calculated intensities in the database of H_2S absorption

Intensity, cm^{-2} · atm^{-1}	Species	Band type	Accuracy, %	Region, cm^{-1}
$I > 10^{-4}$	32	cold	< 5	4470–6700
$5 \cdot 10^{-6} < I \le 10^{-4}$	32	cold	≤ 10	
$10^{-6} < I \le 5 \cdot 10^{-6}$	32	cold	< 20	
$I \le 10^{-6}$	32	cold	≥ 20	
All intensities	32	hot	≥ 20	
$I > 5 \cdot 10^{-5}$	33,34	cold	≤ 10	
$5 \cdot 10^{-6} < I \le 5 \cdot 10^{-5}$	33,34	cold	< 20	
$I \le 5 \cdot 10^{-6}$	33,34	cold	≥ 20	
All intensities	32,33,34	cold	≥ 20	7050–8040

The content of the database is shown graphically in Fig. 3. The database includes about 29 000 rotational-vibrational transitions of $H_2{}^{32}S$, $H_2{}^{33}S$, and $H_2{}^{34}S$ to 59 upper vibrational states. Table 6 presents the centers and integral intensities of the bands included into the database, as well as the number of lines for these bands. Note that the integral intensities of the weak $H_2{}^{32}S$ bands (042)–(000), (240)–(000), (231)–(000), (132)–(000) formed by transitions to the dark states are estimated as sums of individual lines borrowing their intensity from stronger lines – resonance partners.

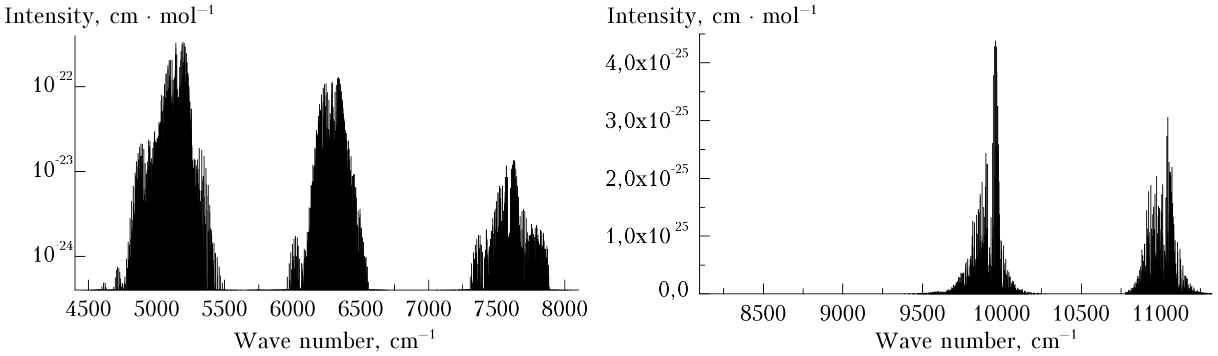

a *b*

Fig. 3. Synthetic absorption spectrum of hydrogen sulfide in the region from 4400 to 11400 cm^{-1}: log (*a*) and linear (*b*) scales.

Table 6. Content of the database on H_2S absorption in the 4400–11400 cm^{-1} region

State		$H_2{}^{32}S$			$H_2{}^{33}S$		$H_2{}^{34}S$	
upper	lower							
$V_1\ V_2\ V_3$	$V_1\ V_2\ V_3$	Band center, cm^{-1}	Integral intensity, cm · mol^{-1}	Line number	Integral intensity, cm · mol^{-1}	Line number	Integral intensity, cm · mol^{-1}	Line number
0 4 0	0 0 0	4661.673	$4.92 \cdot 10^{-23}$	535				
1 2 0	0 0 0	4932.699	$5.19 \cdot 10^{-22}$	844			$1.64 \cdot 10^{-23}$	216
0 2 1	0 0 0	4939.104	$1.58 \cdot 10^{-21}$	1169	$7.94 \cdot 10^{-24}$	166	$6.55 \cdot 10^{-23}$	454
2 1 0	0 1 0	5105.569	$2.64 \cdot 10^{-23}$	326				
1 1 1	0 1 0	5106.596	$6.13 \cdot 10^{-23}$	403				
2 0 0	0 0 0	5144.986	$8.81 \cdot 10^{-21}$	1636	$5.58 \cdot 10^{-23}$	298	$3.61 \cdot 10^{-22}$	627
1 0 1	0 0 0	5147.220	$1.86 \cdot 10^{-20}$	1886	$1.21 \cdot 10^{-22}$	392	$8.17 \cdot 10^{-22}$	915
0 0 2	0 0 0	5243.101	$1.76 \cdot 10^{-21}$	1220	$7.32 \cdot 10^{-24}$	143	$7.01 \cdot 10^{-23}$	448
0 5 0	0 0 0	5797.235	$6.39 \cdot 10^{-24}$	203				
1 3 0	0 0 0	6074.581	$9.03 \cdot 10^{-23}$	566			$1.87 \cdot 10^{-24}$	80
0 3 1	0 0 0	6077.595	$8.32 \cdot 10^{-23}$	541			$4.41 \cdot 10^{-25}$	17
2 2 0	0 1 0	6237.339	$1.04 \cdot 10^{-23}$	248				
1 2 1	0 1 0	6237.515	$3.49 \cdot 10^{-23}$	380				
2 1 0	0 0 0	6288.146	$2.23 \cdot 10^{-21}$	1484	$1.33 \cdot 10^{-23}$	229	$9.74 \cdot 10^{-23}$	567
1 1 1	0 0 0	6289.173	$7.96 \cdot 10^{-21}$	1423	$6.09 \cdot 10^{-23}$	432	$3.47 \cdot 10^{-22}$	743
0 1 2	0 0 0	6385.299	$4.99 \cdot 10^{-23}$	127	$2.17 \cdot 10^{-25}$	6	$1.86 \cdot 10^{-24}$	21
2 2 0	0 0 0	7419.916	$2.04 \cdot 10^{-23}$	198				
1 2 1	0 0 0	7420.092	$1.28 \cdot 10^{-22}$	539				
2 0 1	0 0 0	7526.545	$6.40 \cdot 10^{-22}$	794				
1 0 2	0 0 0	7576.381	$1.86 \cdot 10^{-22}$	601				
3 0 0	0 0 0	7752.264	$2.09 \cdot 10^{-22}$	601				
0 0 3	0 0 0	7779.319	$1.33 \cdot 10^{-22}$	560				
0 4 2	0 0 0	9647.774	$5.31 \cdot 10^{-26}$	17				
2 4 0	0 0 0	9744.888	$2.77 \cdot 10^{-27}$	6				
2 2 1	0 0 0	9806.667	$3.45 \cdot 10^{-24}$	656			$7.19 \cdot 10^{-26}$	111
1 2 2	0 0 0	9806.733	$1.50 \cdot 10^{-24}$	492			$1.23 \cdot 10^{-26}$	24
1 4 1	0 0 0	9847.167	$4.68 \cdot 10^{-25}$	385				
2 0 2	0 0 0	9911.023	$5.91 \cdot 10^{-24}$	840	$5.53 \cdot 10^{-27}$	16	$1.37 \cdot 10^{-25}$	122
3 0 1	0 0 0	9911.023	$2.01 \cdot 10^{-23}$	1074				
2 3 1	0 0 0	10905.790	$1.48 \cdot 10^{-26}$	11				
1 3 2	0 0 0	10905.790	$1.33 \cdot 10^{-26}$	10				
3 1 1	0 0 0	11008.652	$1.42 \cdot 10^{-23}$	902	$3.68 \cdot 10^{-26}$	54	$5.80 \cdot 10^{-25}$	352
2 1 2	0 0 0	11008.680	$8.44 \cdot 10^{-24}$	996	$1.91 \cdot 10^{-26}$	33	$3.34 \cdot 10^{-25}$	287
3 3 0	0 0 0	11097.161	$2.23 \cdot 10^{-25}$	232				

Note: The total number of lines in the database is 28992.

Conclusion

The detailed database of the H_2S absorption lines in the region from 4400 to 11400 cm^{-1} compiled includes about 29 000 rotational-vibrational transitions to 59 upper vibrational states of $H_2{}^{32}S$, $H_2{}^{33}S$, and $H_2{}^{34}S$ molecules. This information can be used in applied problems on hydrogen sulfide detection. The synthetic $H_2{}^{32}S$ spectrum is presented in a convenient format and can be included in the existing spectroscopic databanks, such as HITRAN and GEISA.

Acknowledgments

This work was supported, in part, by the Russian Foundation for Basic Research (Grant No. 02–07–90139)

References

1. L.R. Brown, O.V. Naumenko, E.R. Polovtseva, and L.N. Sinitsa, J. Mol. Spectrosc. (2003) (to be submitted).
2. L.R. Brown, O.V. Naumenko, E.R. Polovtseva, and L.N. Sinitsa, Proc. SPIE **5311**, 58–66 (2003).
3. L.R. Brown, O.V. Naumenko, E.R. Polovtseva, and L.N. Sinitsa, Proc. SPIE **5396**, Part A, 42–48 (2003).
4. Y. Ding, O. Naumenko, Shui-Ming Hu, Ongshi Zhu, E. Bertseva, and A. Campargue, J. Mol. Spectrosc. **217**, 222–238 (2003).
5. O. Naumenko and A. Campargue, J. Mol. Spectrosc. **209**, 242–253 (2001).
6. A. Bykov, O. Naumenko, M. Smirnov, L. Sinitsa, L. Brown, J. Crisp, and D. Crisp, Can. J. Phys. **72**, 989–1000 (1994).
7. A.D. Bykov, O.V. Naumenko, A.M. Pshenichnikov, L.N. Sinitsa, and A.P. Shcherbakov, Opt. Spektrosk. **94**, 528–537 (2003).
8. J-M. Flaud and C. Camy-Peyret, Can. J. Phys. **61**, 1462–1473 (1983).
9. O. Naumenko and A. Campargue, J. Mol. Spectrosc. **210**, 224–232 (2001).
10. V. Tyuterev, S. Tashkun, and D. Schwenke, Chem. Phys. Lett. **348**, 223–234 (2001).
11. L. Lechuga-Fossat, J.-M. Flaud, C. Camy-Peyret, P. Arcas, and M. Cuisenier, J. Mol. Phys. **61**, No. 1, 23–32 (1987).
12. C. Camy-Peyret and J.-M. Flaud, in: *Molecular Spectroscopy: Modern Research*, ed. by K. Narahari Rao, (Academic Press, New York, 1985), Vol. III, pp. 69–109.